Localization as a consequence of quasiperiodic bulk-bulk correspondence

Dan S. Borgnia[1,*] and Robert-Jan Slager[2,1,†]

[1]*Department of Physics, Harvard University, Cambridge, Massachusetts 02138, USA*

[2]*TCM Group, Cavendish Laboratory, University of Cambridge, J. J. Thomson Avenue, Cambridge CB3 0HE, United Kingdom*

(Received 27 December 2021; revised 23 June 2022; accepted 23 January 2023; published 8 February 2023)

We report on a direct connection between band theory, quasiperiodic topology, and the almost-Mathieu (Aubry-André) metal insulator transition (MIT). By constructing the transfer matrix equations of one-dimensional (1D) quasiperiodic operators from rational approximate projected Green's functions, we relate the quasiperiodic Lyapunov exponents to the chiral edge modes of rational-flux Hofstadter Hamiltonians. We thereby show that the insulating phase is rooted in a topological "bulk-bulk" correspondence, a bulk-boundary correspondence between the 1D Aubry-André system (boundary) and its two-dimensional (2D) parent Hamiltonian (bulk). We extend this connection to random disorder via a Fourier expansion in quasiperiodic modes, demonstrating our results are widely applicable to systems beyond this paradigmatic model. The uncorrelated disorder limit is characterized by the breakdown of bulk-boundary driven quasiperiodic localization.

DOI: 10.1103/PhysRevB.107.085111

I. INTRODUCTION

Quasiperiodic systems have played and continue to play a prominent role in condensed matter physics [1–9]. The Aubry-André-Harper (AAH) model, or the almost-Mathieu operator in the mathematics community, is the prototypical example of quasiperiodic systems. In contrast to periodic or randomly disordered systems, the AAH model hosts many exotic properties, including a metal insulator transition (MIT), a well-established duality between the two phases [10–12], and a connection to a two-dimensional (2D) quantum Hall system on a lattice, nearest neighbor (n.n.) Hofstadter model. Here, we report a new relation between this 2D quasiperiodic topology, the famous metal insulator transition, and translation-invariant band topology—we directly compute the Lyapunov exponents and corresponding spectral measure using the constraint of bulk-boundary correspondence in the 2D Harper Hamiltonian. This complements existing works showing the existence of edge modes [1,2,13,14], promoting this topological constraint on the existence of edge modes to a bulk-bulk correspondence.

Following the ideas in Ref. [15] and constructing a sequence of *rational approximate* transfer matrix equations (TMEs) from projected Green's functions (pGFs), we construct an explicit map between the dynamical invariants from $SL(2,\mathbb{R})$ cocycle theory [16–21] describing the eigenfunction localization and higher dimensional band topological invariants. In particular, we show that the quasiperiodic localization is an exotic example of bulk-boundary correspondence where 1D bulk localized states reflect a virtual 2D bulk topological invariant; see Table I. This behavior does not occur with random disorder as nontrivial Chern markers are incompatible with localization [22], adding to the repertoire of exotic quasiperiodic phenomena. Indeed, random disorder is the multimodal quasiperiodic limit for which this correspondence fails [15].

We proceed by reviewing the AAH model including the connection between the one-dimensional (1D) AAH model and the 2D Hofstadter model [1,2,11,23–25] and the metal insulator transition [16–21]. We then construct 2D rational approximate TMEs following Ref. [15] and link 2D chiral topological edge modes to a lack of 1D TME solutions by computing bulk Lyapunov exponents. We conclude with a comparison to random disorder.

II. ALMOST-MATHIEU REVIEW

When we set $\Theta = 2\pi\alpha$ and $\alpha \in \mathbb{R} - \mathbb{Q}$, the AAH Hamiltonian takes the form

$$\hat{H} = \sum_x t(\hat{c}^\dagger_{x+1}\hat{c}_x + \hat{c}_{x+1}\hat{c}^\dagger_x) + 2V\cos(\Theta x + \delta_y)\hat{c}^\dagger_x\hat{c}_x. \quad (1)$$

Considering Eq. (1) as a Landau gauge of a 2D tight binding model with irrational flux per plaquette Θ and the

TABLE I. For diophantine α, the table lists AAH phases, the convergent 2D Hamiltonian Landau gauge, and number of TME discontinuities per spectral gap from chiral edge modes.

	Horizontal	Vertical	Phase	Discontinuities
$V < t$	Yes	No	Metal	One
$V > t$	No	Yes	Insulator	All
$V = t$	Yes/no	Yes/no	Transition	N/A

*dbognia@g.harvard.edu
†rjs269@cam.ac.uk

y-momentum δ_y uncovers a topological gap structure [1,15],

$$\mathcal{H}_{2D}(\Theta) = \sum_{x,\delta_y} t\hat{c}^\dagger_{x+1,\delta_y}\hat{c}_{x,\delta_y} + t^*\hat{c}^\dagger_{x,\delta_y}\hat{c}_{x+1,\delta_y} + 2V\cos(\Theta x + \delta_y)\hat{c}^\dagger_{x,\delta_y}\hat{c}_{x,\delta_y}. \quad (2)$$

Varying Θ produces the Hofstadter butterfly, Fig. 3, with gaps labeled by integers, $\{m + n\Theta | m, n \in \mathbb{Z}\}$, the gap-labeling theorem [1,15,24,26]. The MIT is understood through the corresponding transfer matrix equation (TME) for Eq. (1) ($t = 1$),

$$\overbrace{\begin{pmatrix} E - 2V\cos(\Theta x + \delta_y) & -1 \\ 1 & 0 \end{pmatrix}}^{\hat{T}^{E,V}_{\alpha,x}(\delta_y)} \begin{pmatrix} \psi_x \\ \psi_{x-1} \end{pmatrix} = \begin{pmatrix} \psi_{x+1} \\ \psi_x \end{pmatrix}. \quad (3)$$

A cocycle $(\alpha, A^E_V(\delta_y))$ is generated from the irrational parameter α and corresponding $A^E_V(\delta_y + \Theta x) = \hat{T}^{E,V}_{\alpha,x}(\delta_y) \in \mathrm{SL}(2, \mathbb{R})$. Lyapunov exponents are defined as

$$L^V(E, \alpha) = \lim_{n\to\infty}\left[\frac{1}{n}\int_0^{2\pi} \ln\left|\left|\prod_{x=1}^{n} A^E_V(\delta_y + \Theta x)\right|\right|\frac{d\delta_y}{2\pi}\right], \quad (4)$$

where $||A|| = \sup_{\psi\in\mathcal{H}}(||A\psi||/||\psi||)$ is the operator norm. Lyapunov exponents characterize the log growth of transfer matrix eigenvalues (normalization of eigenfunctions) with $L^V(E, \alpha) = 0$ corresponding to extended TME solutions [17,27]. They are continuous in V [27], can be analytically continued, $\delta_y \to \delta_y + i\epsilon \Rightarrow L^V(E, \alpha) \to L^V_\epsilon(E, \alpha)$, and have quantized acceleration [28],

$$\omega^V(E, \alpha) = \lim_{\epsilon\to 0^+}\frac{1}{2\pi\epsilon}\left(L^V_\epsilon(E, \alpha) - L^V(E, \alpha)\right). \quad (5)$$

The acceleration forms a discretization of almost-Mathieu dynamics and was used to prove the phase diagram [28]; i.e., the spectrum is as follows (see Appendix A):

(1) Absolutely continuous (metallic) for all Θ and all δ if $V < t$; $L^V(E, \alpha) = 0$ for $E \in \Sigma$.

(2) Singularly continuous (critical) for all Θ and all δ if $V = t$; $L^V(E, \alpha) = 0$, $\omega^V(E, \alpha) = 1$ for $E \in \Sigma$.

(3) Pure pointlike (insulator) for almost all Θ and almost all δ if $V > t$; $L^V(E, \alpha) = \ln(V/t)$ for $E \in \Sigma$.

References [19,29,30] connected this dynamical classification to the gap-labeling theorem, topological invariants of the almost-Mathieu spectral gaps [24].

III. RATIONAL APPROXIMATES

We connect the almost-Mathieu spectral gaps to rational flux lattice Integer quantum Hall effect (IQHE) gaps (band topology) through a sequence of transfer matrix equations (TMEs) constructed by substituting $\Theta = 2\pi\alpha$ in Eq. (2) with its Nth continued fraction approximation $\Theta_N = 2\pi\, p_N/q_N$,

$$\frac{p_N}{q_N} = a_0 + 1/\{a_1 + 1/[a_2 + 1/(\cdots + 1/a_N)]\}. \quad (6)$$

Following Ref. [15], we consider two different regimes: $V < t$ and $V > t$ (for α diophantine).

IV. HORIZONTAL UNIT CELL ($V < t$)

For each δ_y, consider $H_{N,\delta_y} = \mathcal{H}_{2D}(\Theta_N)|_{\delta_y}$ and define a q_N-site unit cell in the x direction,

$$\Psi^{\delta_y}_{x,N} = \begin{pmatrix} \psi_{xq_N+1,\delta_y} & \cdots & \psi_{xq_N+q_N,\delta_y} \end{pmatrix}^T, \quad (7)$$

the projected Green's function (pGF) onto one unit cell,

$$G_N(E, \delta_y) = \Psi^{\delta_y,\dagger}_{x,N}\left(E - H_{N,\delta_y}\right)^{-1}\Psi^{\delta_y}_{x,N}, \quad (8)$$

and a corresponding TME (setting $t = 1$),

$$\overbrace{\frac{1}{G^{1,q_N}_N(E, \delta_y)}\begin{pmatrix} 1 & -G^{q_N,q_N}_N(E, \delta_y) \\ G^{1,1}_N(E, \delta_y) & G^{q_N,1}_N(E, \delta_y)G^{1,q_N}_N(E, \delta_y) - G^{1,1}_N(E, \delta_y)G^{q_N,q_N}_N(E, \delta_y) \end{pmatrix}}^{\hat{T}^{E,V}_{q_N,q_Nx}(\delta_y)} \begin{pmatrix} \psi_{q_Nx+1,\delta_y} \\ \psi_{q_Nx,\delta_y} \end{pmatrix} = \begin{pmatrix} \psi_{q_N(x+1)+1,\delta_y} \\ \psi_{q_N(x+1),\delta_y} \end{pmatrix} \quad (9)$$

with $G^{i,j}_N(E, \delta_y) = \langle i|\, G_N(E, \delta_y)\, |j\rangle$, $\{i, j \in (1, \ldots, q_N)\}$.

For $V < t$, the (operator norm) difference between the rational pGF and the full irrational Green's function vanishes as $q_N \to \infty G_N(E, \delta_y) = G_\alpha(E, \delta_y)$ [15], such that Eq. (9) is just q_N applications of Eq. (3) as $q_N \to \infty$. We project to the 1D Hamiltonian in Eq. (1) by fixing δ_y (Fig. 1), and compute the Lyapunov exponents,

$$L^V(E, \alpha) = \lim_{q_N\to\infty}\left[L^V\left(E, \frac{p_N}{q_N}\right)\right]. \quad (10)$$

In Eq. (9), if $G^{1,1}_N(E, \delta_y) \neq 0$ and $G^{q_N,q_N}_N(E, \delta_y) \neq 0$, $\hat{T}^{E,V}_{q_N,x}(\delta_y)$ is unitary and has reciprocal eigenvalues, $\lambda_{T,1}\lambda_{T,2} = 1$. The spectrum, $E \in \Sigma_{H_N}$, is formed by energies for which $|\lambda_T| = 1$. Energies for which $|\lambda_T| \in (0, 1) \cup (1, \infty)$ form the spectral gaps, $E \in \mathbb{R} - \Sigma$; Fig. 1. Thus, for all $E \in \Sigma_{H_N}$, $L^V(E, \alpha)$ and $\omega^V(E, \alpha) = 0$, and for $E \notin \Sigma_{H_N}$, $L(E, \alpha) > 0$.

If $\det G_N(E, \delta_y) = 0$, then by the convergence argument in Ref. [15] and Appendix D, $||\hat{T}^{E,V}_{q_N,x}(\delta_y)|| > (t/V)^{q_N}$ and $L(E, \frac{p_N}{q_N}) > \ln(t/V)$, i.e., a bound state of the half-infinite chain. The rational Lyapunov exponents are continuous in E, V [27] and converge to zero for $E \in \Sigma_{H_\alpha}$, forming an absolutely continuous spectrum (by excluding the pure-point spectrum).

The bound states, generated by zeros of $\det G_N(E, \delta_y)$, arise from topological winding of the bulk Green's function in Eq. (8) [31–39], correspond to edge modes, and are a direct consequence of bulk-boundary

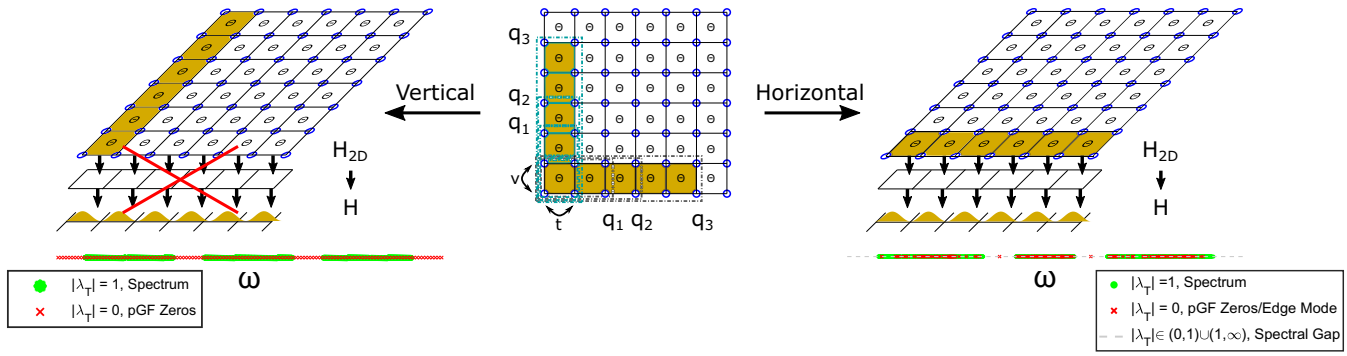

FIG. 1. Top panels (taken from Ref. [15]) shows magnetic unit cells chosen in the 2D parent Hamiltonian (center). For diophantine α in Eq. (2), the regimes $V < t$ and $V > t$ dictate a horizontal or vertical cell respectively. Bottom panel shows the transfer matrix eigenvalues, the corresponding numerically computed AAH spectrum (green), corresponding spectral gaps (grey), and 2D pGF zeros (red cross) for parameters $t = 1, N = 2048, \alpha = \frac{1}{2}(\sqrt{5}-1)$, and $V = 2$ (left) or $V = 0.5$ (right). The spectrum (green) has transfer matrix eigenvalues on the unit circle, $|\lambda_T| = 1$. Zero eigenvalues of the pGF (red cross) imply the transfer matrix is rank deficient, $\lambda_T = 0$. Note the many small gaps (gray) and zeros in every gap (right), and the continuum of rank-deficient points (left).

correspondence in the rational approximate models [15,32,36,39]. While they do not contribution to the bulk Lyapunov exponents, the presence of boundary fixes the gauge choice δ_y, and the corresponding edge mode is formed [1,40].

V. VERTICAL UNIT CELL ($V > t$)

For each Θ_N, Fourier transform the vertical Landau gauged Hamiltonian along the x coordinate, $\hat{c}_{x,y} = \sum_{k_x} e^{ik_x x}\hat{c}_{k_x,y}$, build a unit cell along the y coordinate of size q_N, and Fourier transform into the δ_y basis [15],

$$\tilde{\mathcal{H}}_{2D} = \sum_{\delta_y,k_x}\left[\sum_{n=1}^{q_N}\left(2t\cos(\Theta_N n + k_x)\hat{c}^\dagger_{n,\delta_y,k_x}\hat{c}_{n,\delta_y,k_x} + V\hat{c}^\dagger_{n+1,\delta_y,k_x}\hat{c}_{n,\delta_y,k_x}\right) + Ve^{i\delta_y}\hat{c}^\dagger_{N,\delta_y,k_x}\hat{c}_{1,\delta_y,k_x} + h.c.\right], \tag{11}$$

with $H_{N,k_x} = \tilde{\mathcal{H}}_{2D}(\Theta_N)|_{k_x}$ for each k_x. Then, define a q_N-site unit cell on the xth lattice site,

$$\Psi^{\delta_y}_{x,N} = \left(\psi_{1,x}\ \ldots\ \psi_{q_N,x}\right)^T, \tag{12}$$

the projected Green's function (pGF) onto one unit cell,

$$G_N(E,\delta_y) = \Psi^{\delta_y,\dagger}_{x,N}(E - \tilde{H}_{2D})^{-1}\Psi^{\delta_y}_{x,N},$$
$$G_N(E,\delta_y) = \int_0^{2\pi}\frac{dk_x}{2\pi}\left(E - H_{N,k_x}\right)^{-1}, \tag{13}$$

and the corresponding TME ($t = 1$),

$$\overbrace{\begin{pmatrix} G_N^{-1}(E,\delta_y) & -\mathbb{1}_{q_N} \\ \mathbb{1}_{q_N} & 0\end{pmatrix}}^{\hat{T}^{E,V}_{q_N,x}(\delta_y)}\begin{pmatrix}\Psi^{\delta_y}_{x,N}\\ \Psi^{\delta_y}_{x-1,N}\end{pmatrix} = \begin{pmatrix}\Psi^{\delta_y}_{x+1,N}\\ \Psi^{\delta_y}_{x,N}\end{pmatrix}. \tag{14}$$

We again project back to the 1D Hamiltonian by fixing δ_y; see Fig. 1. However, following Ref. [28], we write $x \to x+1$ as $\delta_y \to \delta_y + \Theta x$ such that

$$\frac{1}{n}\ln\left|\left|\prod_{x=1}^{n}\hat{T}^{E,V}_{q_N,x}(\delta_y)\right|\right| = \ln\left|\left|\prod_{x=1}^{n}\hat{T}^{E,V}_{q_N,0}(\delta_y + \Theta x)\right|\right|^{\frac{1}{n}} \tag{15}$$

and the rational Lyapunov exponents is

$$L^V\left(E,\frac{p_N}{q_N}\right) = \lim_{n\to\infty}\int_0^{2\pi}\frac{d\delta_y}{2\pi}\ln\left|\left|\left(\hat{T}^{E,V}_{q_N,0}(\delta_y)\right)^n\right|\right|^{\frac{1}{n}}, \tag{16}$$

where all δ_y contribute.

Notice, bulk-boundary correspondence [1,41] guarantees the 2D rational approximates will host edge modes corresponding to the nontrivial magnetic flux per plaquette (the IQHE), and for $\forall E$, $\exists\delta_y^E$ such that $\det G_N(E,\delta_y^E) = 0$ in Eq. (13); see Fig. 2. Thus,

$$L^V\left(E,\frac{p_N}{q_N}\right) \geqslant \begin{cases}0, & \text{if } E \in \Sigma_{H_N}\\ \ln(V/t), & \text{if } E \notin \Sigma_{H_N}\end{cases}. \tag{17}$$

The rational Lyapunov exponents, $L^V(E,\frac{p_N}{q_N})$, must be jointly continuous in E, V as $q_N \to \infty$ [27]. The irrational spectrum, Σ_{H_α}, must have zero overlap with the complement of the rational spectra, $\lim_{q_N\to\infty}\bar{\Sigma}_{H_N}$. Thus, the Lyapunov exponents must converge to $L^V(E,\alpha) = V$ for $E \in \Sigma_{H_\alpha}$, as the spectrum is a cantor set (nowhere dense) [19]. This implies the absence of an absolutely continuous spectrum, i.e., a pure-point-like spectrum (up to singular continuous contributions [16]).

We make this explicit using the ideas in Refs. [15,28]. The Lyapunov exponents, $L^V(E,\alpha)$, are computed away from the real axis with $\delta_y \to \delta_y + i\epsilon$ for $\epsilon > 0$, such that $L^V_\epsilon(E,\frac{p_N}{q_N})$ is almost everywhere (a.e.) continuous. By Refs. [8,15,28], for any $\epsilon > 0$ and large enough q_N,

$$\det(E - H_{N,\delta_y+i\epsilon}) = \det(E - H_{N,\delta_y}) + (-Ve^{2\pi\epsilon})^{q_N}. \tag{18}$$

Thus, for $E \in \Sigma_{H_N}$, $\det(E - H_{N,\delta_y}) = 0$ and

$$\left|\left|\left(\hat{T}^{E,V}_{q_N,0}(\delta_y)\right)^{q_N}\right|\right|^{1/q_N} = Ve^{2\pi\epsilon}, \tag{19}$$

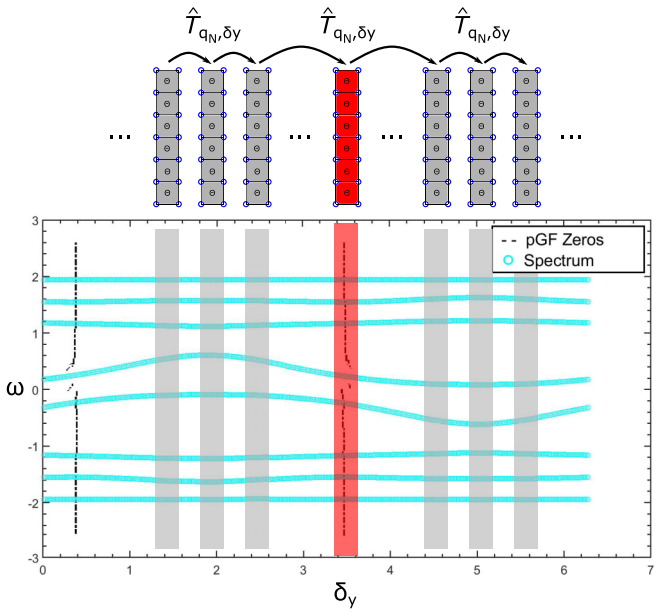

FIG. 2. (Top) Concatenated transfer matrices for vertical unit cells. For each ω there exists a δ_y such that $\det(\hat{T}_{q_N,\delta_y}) = 0$; (bottom) rational approximate pGF zeros plotted as a function of δ_y (k_y) for $q_N = 8$ in golden mean approximation. Notice the presence of a zero for each energy (up to numerical precision) in the spectral gaps.

taking $t = 1$. Then, Eq. (16) reduces to

$$L_\epsilon^V\left(E, \frac{p_N}{q_N}\right) = \ln(V) + 2\pi\epsilon. \tag{20}$$

Consistent with Ref. [28], this implies for $E \in \Sigma_{H_N}$,

$$L_\epsilon^V(E,\alpha) = \lim_{q_N\to\infty} L_\epsilon^V(E,\alpha) = \ln(V), \tag{21}$$

$$\omega^V(E,\alpha) = \lim_{N\to\infty} \omega^V\left(E, \frac{p_N}{q_N}\right) = 1, \tag{22}$$

such that the spectrum is localized [28].

VI. TOPOLOGICAL LOCALIZATION

The transition from a convergent horizontal unit cell to a convergent vertical unit cell [15] corresponds to a localization transition and bulk-boundary correspondence—the quasiperiodic bulk topology and the corresponding chiral edge modes—forces bulk localization, a "bulk-bulk" correspondence. In contrast, the Fibonacci quasicrystal lacks bulk-boundary correspondence [1,26] and, consistent with the discussion above, is power-law (not exponentially) localized for any parameter regime [42,43].

A similar argument can be applied to uncorrelated disorder and 1D Anderson localization. Consider a n.n. Hamiltonian with an on-site potential generated from the uniform distribution $\{V_x \in (-V, V)\}$, $\hat{V} = \sum_x V_x \hat{c}_x^\dagger \hat{c}_x$, and Fourier decompose V_x in a quasiperiodic basis,

$$V_x = \sum_n [V_n e^{i(2\pi\alpha n x + n\delta_y)} + V_n^* e^{-i(2\pi\alpha n x + n\delta_y)}] \tag{23}$$

The corresponding 2D multimodal quasiperiodic Hamiltonian is n.n. in the horizontal direction and $\sim\frac{1}{a}$ range in the vertical direction (lattice constant a),

$$\hat{\mathcal{H}}_{x,y} = t\hat{c}_{x+1,y}^\dagger \hat{c}_{x,y} + \sum_n [V_n e^{i(2\pi\alpha n x)} \hat{c}_{x,y+n}^\dagger \hat{c}_{x,y}] + t^* \hat{c}_{x,y}^\dagger \hat{c}_{x+1,y} + \sum_n [V_n^* e^{-i(2\pi\alpha n x)} \hat{c}_{x,y}^\dagger \hat{c}_{x,y+n}]. \tag{24}$$

These long-range hopping models have subtle phase diagrams beyond the scope of this article, especially in the limit when hopping magnitudes decay slowly [44,45]. Instead, we consider a prime number high-pass filter, choosing a prime P such that $V_n = 0$ for all $|n| > P$, and taking the limit as $P \to \infty$. For all $q_N > P$, define a $(q_N \times P)$-dimensional unit cell such that all sites are effectively n.n. coupled, the flux per unit cell is zero, and Eq. (14) applies. Then, by choosing P large enough for a given V, the rational Lyapunov exponents take the same form as in Eq. (17), a.e. discontinuous. By similar arguments as above, the irrational spectrum, Σ_{H_α}, must be pure-point like and localized. The finite-frequency, random disorder localization defines a natural limit from single-mode quasiperiodic systems to uncorrelated disorder and provides insight into the stability of Anderson localization in finite-size systems.

The uncorrelated disorder limit corresponds precisely to the breakdown of the quasiperiodic construction due to nondecaying long-range hopping. In the $P \to \infty$ limit, the spectral gaps are not guaranteed to stay open, Chern markers must be trivial [22], and the convex hull generated by the disorder pattern (Refs. [1,26]) is deformable to a point such that the the bulk-boundary correspondence argument leading to Eq. (17) does not apply. The gap closings separate quasiperiodic systems from disorder as the integrated density of states is no longer quantized [19,24,46] and the Lyapunov exponents can vary with energy. We leave the exploration of this limit to future work.

VII. CONCLUSIONS

In summary, we report that the quasiperiodic metal insulator transition is the consequence of bulk-boundary correspondence and quasiperiodic topology, generated by the chiral edge modes of the rational approximates, and connect band topology to the metal insulator transition. This makes precise the intuition presented by Aubry and André in [10,47] that the MIT resembles a $U(1)$ gauge-symmetry-breaking transition. The metallic eigenfunctions are invariant under phase shifts of the AAH on-site potential, a gauge freedom of the TME in Eq. (9), and the corresponding Lyapunov exponents are not averaged over the phase δ_y. By contrast, there is no such gauge freedom in the 1D transfer matrix in Eq. (14), and the corresponding Lyapunov exponents are averaged over all phases δ_y. The self-interference generates localized eigenfunctions.

In practice, the construction generalizes to 1D quasiperiodic patterns with bulk-boundary correspondence, even if not analytically tractable, by the methods in Ref. [15] and the gap labeling for virtual topological invariants in Ref. [26]. Indeed, we extend the connection between band topology and eigenfunction localization to uncorrelated disorder via a sequence of long-range hopping models. While similar in numerical simulation due to the finite-size truncation of ran-

dom disorder and resulting finite hopping in Eq. (24), the random disorder limit corresponds to the breakdown of these topological constraints. We leave to future work connections between localization and higher order topological invariants in higher dimensional quasiperiodic systems.w

ACKNOWLEDGMENTS

We cordially thank A. Vishwanath and S. Jitomirskaya for many discussions and advice. We also thank V. B. Bulchandani, R. Verresen, M. Gilbert, N. G. Jones, J. Rodriguez-Nieva, D. Else, I. Petrides, D. E. Parker, E. Borgnia, M. McCann, William E. Conway, S. K. Wilson, W. Vega-Brown, and especially M. Brennan for insightful discussions. R.-J.S. acknowledges funding from the Winton Programme for the Physics of Sustainability and from the Marie Skłodowska-Curie Programme under EC Grant No. 842901 as well as from Trinity College at the University of Cambridge.

APPENDIX A: AAH BACKGROUND

The main results of this work generalize to multiple classes of quasiperiodic models, but the Aubry-André model (almost-Mathieu operator) is the most well studied. We introduce it and some background on current methods in the study of single-particle quasiperiodic models. The Hamiltonian is simple but presents a rich playground for new techniques in analysis and single-particle physics:

$$\hat{H} = \sum_x t(\hat{c}^\dagger_{x+1}\hat{c}_x + \hat{c}_{x+1}\hat{c}^\dagger_x) + 2V\cos(\Theta x + \delta_y)\hat{c}^\dagger_x\hat{c}_x. \quad \text{(A1)}$$

Here $\Theta = 2\pi a$, and we will take $a \in \mathbb{R} - \mathbb{Q}$.

To understand why the almost-Mathieu operator is mathematically interesting, beyond the physically interesting metal-insulator transition, we introduce the notion of a *spectral measure*:

For any self-adjoint linear operator, T, one can decompose its measure on the target Hilbert space, $\mathcal{H}$ as an *absolutely continuous*, *singularly continuous*, and *pure-point-like* components. The spectral measure of T is defined with respect to a vector $h \in \mathcal{H}$ and a positive linear functional $f : T \to \langle h|\, f(T)\,|h\rangle = \int_{\sigma(T)} f d\mu_h$, where $\sigma(T)$ is the spectrum of the operator T and μ_h is the unique measure associated with h and T.

The portion of the Hilbert space, i.e., the subspace of vectors, for which μ_h is dominated by the Lebesgue measure on the same subspace—for every measurable set A, if the Lebesgue measure $L(A) = 0$, $\mu_h(A) = 0$—is absolutely continuous. By contrast, the pure-point-like component is the discrete portion of the spectrum where points can have finite measure in terms of μ_h, but points have zero Lebesgue measure. The singularly continuous part of the spectrum is defined as the singular part of the spectrum—the subspace which can be formed by a disjoint union of sets A and B for which $\mu_h(A) = 0$ when $L(B) = 0$—which is not pure-point-like.

The original metal-insulator transition was shown non-rigorously through the duality of the Aubry-André under a Fourier transform-like operation, $\hat{c}_k = \sum_x \exp(i\Theta kx)\hat{c}_x$,

$$\tilde{\hat{H}} = \sum_k V(\hat{c}^\dagger_{k+1}\hat{c}_k + \hat{c}_{k+1}\hat{c}^\dagger_k) + 2t\cos(\Theta k + \delta_k)\hat{c}^\dagger_k\hat{c}_k; \quad \text{(A2)}$$

see Appendix B. The model has a self-dual point for $V = t$, fixing a transition from momentum-like to position-like eigenfunctions. A more complete formulation of the problem, however, was constructed and proven for almost-Mathieu operators. It was proven that the spectrum of the almost-Mathieu operator is (setting $t = 1$) as follows:

(1) Absolutely continuous for all Θ and δ_x when $V < 1$.
(2) Singularly continuous for all Θ and δ_x when $V = 1$.
(3) Pure-point-like for almost all Θ and δ_x when $V > 1$.

A pure-point-like spectrum guarantees Anderson localization as it corresponds to eigenfunctions having finite measure at the eigenvalues and zero measure elsewhere. Intuitively, only a finite number can effectively participate (exponentially decaying weight) in generating discretely separated eigenvalues, and the eigenfunction is exponentially decaying on the lattice. More formally, the pure-point-like spectrum forces eigenfunctions to be semiuniformly localized eigenstates [48]. By contrast, an absolutely continuous spectrum guarantees delocalization if the spectrum has finite measure, which has been shown to be the case for the almost-Mathieu operator. Much less is known about the singularly continuous case, and it has been the topic of multiple famous problems proposed by Barry Simon [49–51]. One of the few results on the singularly continuous spectrum is its existence deep in the pure-point-like regime for Liouville $a = 2\pi/\Theta$—sequence of rational approximates $\{p_n/q_n\}$ exists such that $|a - p_n/q_n| < n^{-q_n}$ [52]. In fact, for Liouville numbers, the pure-point-like transition occurs for $\lambda = e^\beta$ with $\beta = \lim_{n\to\infty} \ln(q_n)/q_{n+1}$ [20].

In this language, the almost-Mathieu operator becomes a clear bridge between the well-understood Mathieu operator (periodic operators) and random disorder. Understanding localization for the almost-Mathieu operator directly links to our understanding of chaos and localization in disordered systems. Yet, we still do not understand the full parameter space of a 1D nearest neighbor hopping lattice model with a cosine potential. The almost-everywhere part of this problem is important as it determines the physical stability of the model. Modern techniques in the field rely on cocycle theory [16,17,19,27], and the absolutely continuous part of the spectrum is conjectured to be equivalent to the almost-reducibility of the corresponding cocycle [17]. The connection with cocycle theory further highlights the importance of this problem, as the reducibility classes of $SL(2, \mathbb{R})$ cocycles are known to describe the onset of quantum chaos and directly link to the Lyapunov exponent [17,18,27].

APPENDIX B: ANDRÉ-AUBRY'S ARGUMENT

Early studies of quasiperiodic system dynamics focused on the construction of eigenstates from sequences of rational approximates, inductively [11,53]. While the original work by André and Aubry [10] relied on the continuity of the Thouless parameter and self-dual models to explain the transition. The RG-like induction methods proved rigorously the existence of a localized phase. For the AAH model [11,53] and similar quasiperiodic potentials [11], these methods demonstrated the emergence of a *pure-point-like* spectrum for strong enough onsite potentials (relative to hopping terms). A pure-point-like spectrum enforces localized eigenstates as eigenstates lack support across any continuous energy windows [3,11,16,53,54]. Below we introduce the simple AAH

model and note key insights about the breakdown of eigenstate ergodicity.

The original paper by André and Aubry [10] rests on two fundamental requirements for a quasiperiodic Hamiltonian, its self-duality and its fidelity to a sequence of rational approximates. It proposed a Hamiltonian, the AAH model, which satisfies a self-duality constraint under a real-space to dual-space (momentum space in the continuum limit) transformation, $\hat{c}_k = \sum_x \exp(i\Theta kx)\hat{c}_x$:

$$\hat{H} = \sum_x t(\hat{c}^\dagger_{x+1}\hat{c}_x + \hat{c}_{x+1}\hat{c}^\dagger_y) + 2V\cos(\Theta x + \delta_x)\hat{c}^\dagger_x\hat{c}_x, \quad \text{(B1)}$$

$$\tilde{\hat{H}} = \sum_k V(\hat{c}^\dagger_{k+1}\hat{c}_k + \hat{c}_{k+1}\hat{c}^\dagger_k) + 2t\cos(\Theta k + \delta_k)\hat{c}^\dagger_k\hat{c}_k. \quad \text{(B2)}$$

Here Θ is some irrational parameter relative to π and clearly for $t = V$ the Hamiltonian is self-dual, indicating the existence of a transition. One can introduce a sequence of rational approximates, $\{a_n/b_n\}_{n\in\mathbb{N}}$ with $a_n, b_n \in \mathbb{Z}$ and $\lim_{n\to\infty} a_n/b_n = \Theta$. The sequence of Hamiltonians with periodic potentials links the density of states on either side of the duality transformation because there are well-defined bands. One can then write down the corresponding Thouless exponent for each side of the transition:

$$\gamma(E) = \int_{-\infty}^{\infty} \ln|E - E'|dN(E'), \quad \text{(B3)}$$

For rational a_n/b_n, with $t = 1$ and $V = \lambda$, the transformation from Eq. (B1) to Eq. (B2) takes $\tilde{V} \to 1/\lambda$ and $E \to \tilde{E}/\lambda$, which implies $N_{\lambda,k}(E) = \tilde{N}_{1/\lambda,k}(E/\lambda)$ [10]. So,

$$\gamma(E) = \int_{-\infty}^{\infty} \ln\left|\frac{E - E'}{\lambda}\right| d\tilde{N}\left(\frac{E'}{\lambda}\right) + \ln|\lambda|$$

$$\gamma(E) = \tilde{\gamma}\left(\frac{E}{\lambda}\right) + \ln|\lambda|. \quad \text{(B4)}$$

Since quasiperiodic systems do not have bands but rather protected band gaps (discussed below [3,16,54–57]), the Thouless exponent must be non-negative by construction in 1D [10]. Thus, for $\lambda > 1$, $\gamma(E) > 0$ and states are exponentially localized. This all relies on the continuity of the Thouless exponent, only proven in 2002 [27]. Here, the rational approximates differ drastically from the irrational limit, but the density of state is well described by the approximation. In fact, these spectral properties are topologically protected by the quasiperiodic pattern's robustness [1], further expanded below.

Via the above arguments, André and Aubry demonstrated the existence of nonzero Thouless parameter for $V > 1$. And, by the duality of the model, $\gamma(E)$ must be zero for $V < 1$. This transition is unusually sharp, exhibiting exponential localization on either side due to the relation between the Thouless parameters of the self-dual models. Further, the methodology is quite general in 1D and can be extended to other self-dual models, even if the duality is energy dependent [15]. The argument breaks down in higher dimensions as the Thouless exponent is no longer guaranteed to be non-negative [10].

Returning to the Hamiltonian in Eq. (B1), note the phase δ_x sets the "origin" of the pattern. The eigenvalues cannot depend on the phase δ_x in the thermodynamic limit. However, for $\lambda > 1$, if a state of energy E is localized to site x when $\delta_x = 0$, then the state localized to site $x - \delta/\Theta$ has energy E for the shifted Hamiltonian with phase $\delta_x = \delta$. Thus, the eigenstates of each eigenvalue do depend directly on the phase. In Refs. [10,47], this is described as a gauge-group symmetry-breaking transition.

APPENDIX C: AAH ALGEBRA

We follow the work of Prodan [1] in deriving explicit topological invariants in the AAH model context. We construct the unital algebra and use it to label the resulting spectral gaps of the AAH Hamiltonian. Recall that it reads

$$\mathcal{H}_{\delta_x} = \sum_n t\hat{c}^\dagger_{n+1}\hat{c}_n + \text{H.c.} + 2V\cos(\Theta n + \delta_x)\hat{c}^\dagger_n\hat{c}_n, \quad \text{(C1)}$$

in terms of the creation operators $c^\dagger_i$, lattice constant a, and potential V that depends on the position n and is indexed by phase δ_x. The model exhibits a duality under the pseudo-Fourier transformation $c_k = \sum_n \exp(-ikn)c_k$ [10]. Considering $\delta_x = 0$, one obtains

$$\tilde{\mathcal{H}}(k) = \sum_{k,k',n} te^{ik(n+1)-ik'n}\hat{c}^\dagger_k\hat{c}_{k'} + t^* e^{ikn-ik'(n+1)}\hat{c}^\dagger_k\hat{c}_{k'}$$
$$+ V(e^{2\pi ian+i(k-k')n} + e^{-2\pi ian+i(k-k')n})\hat{c}^\dagger_k\hat{c}_{k'},$$
$$\tilde{\mathcal{H}}_\phi = \sum_k 2t\cos(\Theta k)\hat{c}^\dagger_k\hat{c}_k + V(\hat{c}^\dagger_{k+1}\hat{c}_k + \text{H.c.}), \quad \text{(C2)}$$

where in the last line we have set $k = \Theta m$ and defined $\sum_n \exp(i\Theta n(m - m')) = \delta(m - m')$ in the limit $n \to \infty$. A natural equivalence emerges between $\mathcal{H}$ and $\tilde{\mathcal{H}}$ under $V \to t$, implying the model undergoes a transition for $V = t$, being the well-known 1D metal-insulator transition. Considering the limits $V = 0$ and $t = 0$, the duality relates extended (momentum-localized) eigenstates to position-localized states.

The duality in the AAH model has been focus of many localization studies, past and present [3,10]. The model took on new light, however, when the authors of Ref. [2] noticed it could be parameterized by the phase choice δ_x [2,3,18,23]. Naively, this phase choice is irrelevant as it corresponds to a shift in initial position of an infinite chain, but the 2D *parent* Hamiltonian, as function of x and δ_x, has a topological notion. In particular, it corresponds to a 2D tight-binding model with an irrational magnetic flux per plaquette. Explicitly,

$$\mathcal{H} = \sum_{n,\delta_x} t\hat{c}^\dagger_{n+1,\delta_x}\hat{c}_{n,\delta_x} + t^*\hat{c}^\dagger_{n,\delta_x}\hat{c}_{n+1,\delta_x} + 2V\cos(\Theta x + \delta_x)\hat{c}^\dagger_{n,\delta_x}\hat{c}_{n,\delta_x},$$
$$\tilde{\mathcal{H}} = \sum_{n,m,m'} t\delta_{m,m'}(\hat{c}^\dagger_{n+1,m}\hat{c}_{n,m'} + t^*\hat{c}^\dagger_{n,m}\hat{c}_{n+1,m'}) + V(e^{i\Theta x}\delta_{m+1,m'} + e^{-i\Theta x}\delta_{m-1,m'})\hat{c}^\dagger_{n,m}\hat{c}_{n,m'},$$
$$\tilde{\mathcal{H}} = \sum_{n,m} t(\hat{c}^\dagger_{n+1,m}\hat{c}_{n,m} + \hat{c}^\dagger_{n,m}\hat{c}_{n+1,m}) + V(e^{i\Theta n}\hat{c}^\dagger_{n,m+1}\hat{c}_{n,m} + e^{-i\Theta n}\hat{c}^\dagger_{n,m-1}\hat{c}_{n,m}). \quad \text{(C3)}$$

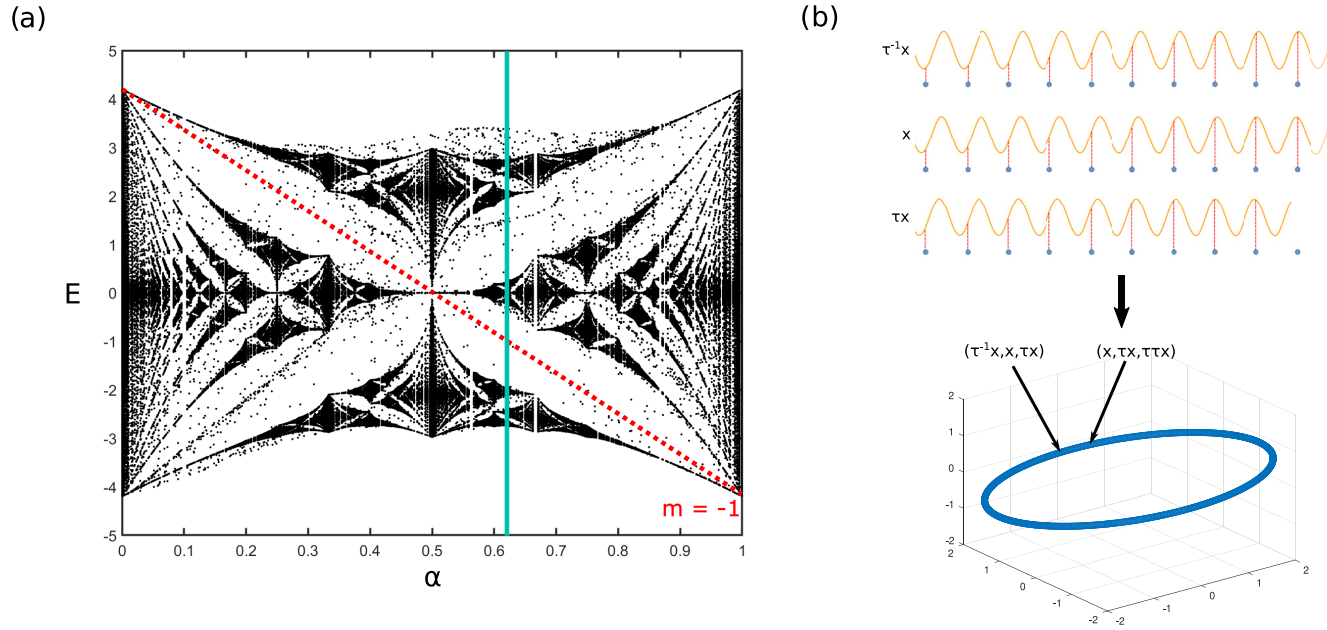

FIG. 3. (a) Quasiperiodic spectrum as function of plaquette flux. Note the gap labeling, where gaps are generated by lines of different slopes—lines curved in spectrum, but straight in Integrated Density of States (IDoS)[1]. (Panel (b) is taken from Ref. [15].) Illustration of quasiperiodic pattern generating a minimal surface (convex hull [1]). This forms the underlying unital algebra, taking the place of a Brillouin zone.

The 2D spectrum amounts to a Hofstadter butterfly when varying the flux per plaquette, Θ. For any rational flux, $\Theta/2\pi = p/q \in \mathbb{Q}$, one can define a magnetic unit cell specifying bands that have a Chern number, which sum to zero, see Fig. 3. This is however not possible for an irrational flux. In this case, strategies outlining sequences of rational approximates, with similar band gaps, to find topological invariants were employed [58].

APPENDIX D: TRANSFER MATRIX COMPUTATIONS

A benefit of the rational approximate transfer matrices is the reduction of a concatenated product of transfer matrices to a 2×2 transfer matrix with four relevant elements: $G_N^{1,q_N}(E,\delta_y)$, $G_N^{q_N,1}(E,\delta_y)$, $G_N^{1,1}(E,\delta_y)$, and $G_N^{q_N,q_N}(E,\delta_y)$. For any rational approximate, these can be computed explicitly. Start with the projected Green's function, but taking the non-Hermitian Peierls phase substitution $te^{i\delta_k} \to te^{i(\delta_k - i\epsilon)}$ and the gauge transformation moving all phases to the corner elements:

$$G_N = \oint_{S^1} \frac{dz}{2\pi i z} \left[E\mathbb{1} - \begin{pmatrix} 2V\cos(\Theta_N + \delta_y) & 1 & 0 & \dots & ze^{iq_N(\delta_k - i\epsilon)} \\ 1 & 2V\cos(\Theta_N 2 + \delta_y) & 1 & \dots & 0 \\ 0 & 1 & 2V\cos(\Theta_N 3 + \delta_y) & \dots & 0 \\ \vdots & \ddots & \ddots & \ddots & \vdots \\ 1/ze^{-iq_N(\delta_k + i\epsilon)} & 0 & \dots & 1 & 2V\cos(\Theta_N q_N + \delta_y) \end{pmatrix} \right]^{-1}. \tag{D1}$$

For any $\epsilon > 0$ there exists a large enough q_N, such that $e^{-q_N\epsilon} < \delta$ for any $\delta > 0$. We can thus ignore the $1/z$ term in what follows even in the limit $\epsilon \to 0$ by choosing first $q_N \to \infty$. It then follows from the cofactor method for computing inverses that

$$G_N^{1,q_N}(E,\delta_y) = \oint \frac{dz}{2\pi i z} \frac{1}{\det\left(E - H_{N,\delta_y}\right)}, \tag{D2}$$

where

$$\det(E - H_{N,\delta_y}) = \det\left[E\mathbb{1} - \begin{pmatrix} 2V\cos(\Theta_N + \delta_y) & 1 & 0 & \dots & ze^{iq_N(\delta_k - i\epsilon)} \\ 1 & 2V\cos(\Theta_N 2 + \delta_y) & 1 & \dots & 0 \\ 0 & 1 & 2V\cos(\Theta_N 3 + \delta_y) & \dots & 0 \\ \vdots & \ddots & \ddots & \ddots & \vdots \\ 0 & 0 & \dots & 1 & 2V\cos(\Theta_N q_N + \delta_y) \end{pmatrix}\right]$$
$$= -(-1)^{q_N+1} z e^{iq_N(\delta_k - i\epsilon)} + [E - 2V\cos(\Theta_N + \delta_y)]\det(E - H_{N,\delta_y})' - \det(E - H_{N,\delta_y})''. \tag{D3}$$

The zeros of $[E - 2V\cos(\Theta_N + \delta_y)]\det(E - H_{N,\delta_y})' - \det(E - H_{N,\delta_y})''$ are the characteristic solutions of H_{N,δ_y}. Indeed, we notice that $\det(E - H_{N,\delta_y})$ is generated by a recursion relation $\det_{n+1} = (E - 2V\cos(\Theta_N(n+1)))\det_n - \det_{n-1}$,which is the same recursion relation for the quasiperiodic transfer matrix equation,

$$\begin{pmatrix} E - 2V\cos(\Theta_N(n) + \delta_y) & -1 \\ 1 & 0 \end{pmatrix}\begin{pmatrix} \det_n \\ \det_{n-1} \end{pmatrix} = \begin{pmatrix} \det_{n+1} \\ \det_n \end{pmatrix}. \tag{D4}$$

However, we have the boundary condition $\det_1 = E - 2V\cos(\Theta_N + \delta_y)$ and $\det_2 = (E - 2V\cos(\Theta_N + \delta_y))(E - 2V\cos(\Theta_N 2 + \delta_y)) - 1$. This is just the semi-infinite transfer matrix equation. We need energies in the band gap of the rational approximates (not characteristic solutions); the remaining solutions to this transfer matrix equation can only come in three distinct forms: Uniformly hyperbolic growth, uniformly hyperbolic decay, and constant norm. The constant norm solutions correspond to bulk states of the infinite transfer matrix equation and are always slightly shifted into the contour by the $i\epsilon$ prescription above. However, we care about energies in the band gaps of the full bulk operator, $E \notin \Sigma$, and we know that $|\det_n| \to 0$ for decaying solutions, i.e., edge modes. Thus, for energies, E_*, such that there exists an edge mode for the operator H_N with semi-infinite boundary conditions, $\det(E - H_{N,\delta_y}) \to 0$. For such E_*, it follows that

$$G_N^{1,q_N}(E_*, \delta_y) = \oint \frac{dz}{2\pi i z}\frac{1}{z} = 0 \tag{D5}$$

and

$$G_N^{q_N,1}(E_*, \delta_y) = \oint \frac{dz}{2\pi i z}\frac{z - \det_{n-2}\left(E_* - H_{N,\delta_y}\right)}{z - \det\left(E_* - H_{N,\delta_y}\right)} \to \oint \frac{dz}{2\pi i z} = 1. \tag{D6}$$

Similarly,

$$G_N^{1,1}(E_*, \delta_y) = G_N^{q_N,q_N}(E_*, \delta_y) \to \oint \frac{dz}{2\pi i z}\frac{1}{z} = 0, \tag{D7}$$

resulting in the transfer matrix equation for E_*,

$$\overbrace{\begin{pmatrix} \left(\frac{t}{V}\right)^{q_N} e^{\epsilon q_N} & -1 \\ 1 & 0 \end{pmatrix}}^{\hat{T}^{E_*,V}_{q_N,q_N x}(\delta_y)}\begin{pmatrix} \psi_{q_N x+1,\delta_y} \\ \psi_{q_N x,\delta_y} \end{pmatrix} = \begin{pmatrix} \psi_{q_N x+q_N+1,\delta_y} \\ \psi_{Q_N x+q_N,\delta_y} \end{pmatrix}, \tag{D8}$$

where the 1,1 entry comes from the convergence condition on $||G_N(E, \delta - y) - G_\alpha(E, \delta_y)||$ from Ref. [15]. By contrast, if $\det(E - H_{N,\delta_y}) \to \infty$ the integrals are nonuniversal and reproduce the effective q_N-site transfer matrix,

$$\hat{T}^{E\neq E_*,V}_{q_N,x}(\delta_y) = \prod_{n=1}^{q_N}\begin{pmatrix} E - 2V\cos(\Theta_N(n) + \delta_y) & -1 \\ 1 & 0 \end{pmatrix}. \tag{D9}$$

Of course, if $\det(E - H_{N,\delta_y}) = 0$, the Green's function does not exist and we must take a small $i\eta$ offset to compute the relevant quantities. For constant norm solutions (the bulk delocalized solutions) we have divergent behavior, but this is consistent with a Green's function pole in the limit $q_N \to \infty$.

[1] E. Prodan, Virtual topological insulators with real quantized physics, Phys. Rev. B **91**, 245104 (2015).

[2] Y. E. Kraus, Y. Lahini, Z. Ringel, M. Verbin, and O. Zilberberg, Topological States and Adiabatic Pumping in Quasicrystals, Phys. Rev. Lett. **109**, 106402 (2012).

[3] S. Jitomirskaya and I. Krasovsky, Critical almost Mathieu operator: Hidden singularity, gap continuity, and the hausdorff dimension of the spectrum, arXiv:1909.04429.

[4] A. Szabo and U. Schneider, Mixed spectra and partially extended states in a two-dimensional quasiperiodic model, Phys. Rev. B **101**, 014205 (2020).

[5] S. J. Ahn, P. Moon, T.-H. Kim, H.-W. Kim, H.-C. Shin, E. H. Kim, H. W. Cha, S.-J. Kahng, P. Kim, M. Koshino *et al.*, Dirac electrons in a dodecagonal graphene quasicrystal, Science **361**, 782 (2018).

[6] S. Spurrier and N. R. Cooper, Semiclassical dynamics, Berry curvature, and spiral holonomy in optical quasicrystals, Phys. Rev. A **97**, 043603 (2018).

[7] S. Iyer, V. Oganesyan, G. Refael, and D. A. Huse, Many-body localization in a quasiperiodic system, Phys. Rev. B **87**, 134202 (2013).

[8] S. Longhi, Topological Phase Transition in Non-Hermitian Quasicrystals, Phys. Rev. Lett. **122**, 237601 (2019).

[9] D. Mao and T. Senthil, Quasiperiodicity, band topology, and moiré graphene, Phys. Rev. B **103**, 115110 (2021).

[10] S. Aubry and G. André, Analyticity breaking and Anderson localization in incommensurate lattices, Ann. Israel Phys. Soc. **3**, 133 (1980).

[11] J. Fröhlich, T. Spencer, and P. Wittwer, Localization for a class of one-dimensional quasi-periodic Schrödinger operators, Commun. Math. Phys. **132**, 5 (1990).

[12] M. Gonçalves, B. Amorim, E. V. Castro, and P. Ribeiro, Hidden dualities in 1d quasiperiodic lattice models, SciPost Phys. **13**, 046 (2022).

[13] L.-J. Lang, X. Cai, and S. Chen, Edge States and Topological Phases in One-Dimensional Optical Superlattices, Phys. Rev. Lett. **108**, 220401 (2012).

[14] S. Ganeshan, J. H. Pixley, and S. Das Sarma, Nearest Neighbor Tight Binding Models with an Exact Mobility Edge in One Dimension, Phys. Rev. Lett. **114**, 146601 (2015).

[15] D. S. Borgnia, A. Vishwanath, and R.-J. Slager, Rational approximations of quasiperiodicity via projected Green's functions, Phys. Rev. B **106**, 054204 (2022).

[16] S. Y. Jitomirskaya, Metal-insulator transition for the almost Mathieu operator, Ann. Math. **150**, 1159 (1999).

[17] A. Avila and R. Krikorian, Reducibility or nonuniform hyperbolicity for quasiperiodic Schrödinger cocycles, Ann. Math. **164**, 911 (2006).

[18] A. Avila and S. Jitomirskaya, Solving the ten martini problem, in *Mathematical Physics of Quantum Mechanics*, edited by J. Asch and A. Joye (Springer, Berlin, 2006), pp. 5–16.

[19] A. Avila and S. Jitomirskaya, The ten martini problem, Ann. Math. **170**, 303 (2009).

[20] A. Avila, J. You, and Q. Zhou, Sharp phase transitions for the almost Mathieu operator, Duke Math. J. **166**, 2697 (2017).

[21] S. Jitomirskaya and C. A. Marx, Analytic quasi-periodic Schrödinger operators and rational frequency approximants, Geometric Functional Anal. **22**, 1407 (2012).

[22] G. Marcelli, M. Moscolari, and G. Panati, Localization implies Chern triviality in non-periodic insulators, arXiv:2012.14407.

[23] J. Bellissard, A. Formoso, R. Lima, and D. Testard, Quasiperiodic interaction with a metal-insulator transition, Phys. Rev. B **26**, 3024 (1982).

[24] J. Bellissard, Gap-labeling theorems, Lect. Notes Phys. **257**, 99 (1986).

[25] A. Connes, D. Sullivan, and N. Teleman, Quasiconformal mappings, operators on Hilbert space, and local formulae for characteristic classes, Topology **33**, 663 (1994).

[26] C. Bourne and E. Prodan, Non-commutative Chern numbers for generic aperiodic discrete systems, J. Phys. A: Math. Theor. **51**, 235202 (2018).

[27] J. Bourgain and S. Jitomirskaya, Continuity of the Lyapunov exponent for quasiperiodic operators with analytic potential, J. Stat. Phys. **108**, 1203 (2002).

[28] A. Avila, Global theory of one-frequency Schrodinger operators I: Stratified analyticity of the Lyapunov exponent and the boundary of nonuniform hyperbolicity, arXiv:0905.3902 (2009).

[29] R. Han, Dry ten martini problem for the non-self-dual extended Harper's model, Trans. Am. Math. Soc. **370**, 197 (2018).

[30] M. Leguil, J. You, Z. Zhao, and Q. Zhou, Asymptotics of spectral gaps of quasi-periodic Schrödinger operators, arXiv:1712.04700 (2017).

[31] G. E. Volovik, *The Universe in a Helium Droplet* (Oxford University Press, Oxford, UK, 2003), Vol. 117.

[32] J.-W. Rhim, J. H. Bardarson, and R.-J. Slager, Unified bulk-boundary correspondence for band insulators, Phys. Rev. B **97**, 115143 (2018).

[33] R.-J. Slager, The translational side of topological band insulators, J. Phys. Chem. Solids **128**, 24 (2019).

[34] R.-J. Slager, A. Mesaros, V. Juričić, and J. Zaanen, Interplay between electronic topology and crystal symmetry: Dislocation-line modes in topological band insulators, Phys. Rev. B **90**, 241403(R) (2014).

[35] R.-J. Slager, A. Mesaros, V. Juričić, and J. Zaanen, The space group classification of topological band-insulators, Nat. Phys. **9**, 98 (2013).

[36] R.-J. Slager, L. Rademaker, J. Zaanen, and L. Balents, Impurity-bound states and Green's function zeros as local signatures of topology, Phys. Rev. B **92**, 085126 (2015).

[37] A. Bouhon, A. M. Black-Schaffer, and R.-J. Slager, Wilson loop approach to fragile topology of split elementary band representations and topological crystalline insulators with time-reversal symmetry, Phys. Rev. B **100**, 195135 (2019).

[38] R. S. K. Mong and V. Shivamoggi, Edge states and the bulk-boundary correspondence in Dirac Hamiltonians, Phys. Rev. B **83**, 125109 (2011).

[39] D. S. Borgnia, A. J. Kruchkov, and R.-J. Slager, Non-Hermitian Boundary Modes and Topology, Phys. Rev. Lett. **124**, 056802 (2020).

[40] G. M. Graf and J. Shapiro, The bulk-edge correspondence for disordered chiral chains, Commun. Math. Phys. **363**, 829 (2018).

[41] Y. Hatsugai, Chern Number and Edge States in the Integer Quantum Hall Effect, Phys. Rev. Lett. **71**, 3697 (1993).

[42] P. A. Kalugin, A. Yu. Kitaev, and L. Levitov, Electron spectrum of a one-dimensional quasicrystal, Sov. Phys. JETP **64**, 410 (1986).

[43] R. B. Capaz, B. Koiller, and S. L. A. de Queiroz, Gap states and localization properties of one-dimensional Fibonacci quasicrystals, Phys. Rev. B **42**, 6402 (1990).

[44] X. Deng, S. Ray, S. Sinha, G. V. Shlyapnikov, and L Santos, One-Dimensional Quasicrystals with Power-Law Hopping, Phys. Rev. Lett. **123**, 025301 (2019).

[45] Z. Xu, X. Xia, and S. Chen, Non-Hermitian Aubry-André model with power-law hopping, Phys. Rev. B **104**, 224204 (2021).

[46] D. S. Borgnia and R.-J. Slager, The dry ten martini problem at criticality, arXiv:2112.06869.

[47] S. Aubry, On the bifurcation of certain KAM tori in the standard mapping, in *Numerical Methods in the Study of Critical Phenomena* (Springer, Berlin, 1981), pp. 79–80.

[48] P. Deift and B. Simon, Almost periodic Schrödinger operators, Commun. Math. Phys. **90**, 389 (1983).

[49] B. Simon, *Fifteen Problems in Mathematical Physics*, Perspectives in Mathematics Vol. 423 (Birkhäuser, Basel, 1984).

[50] B. Simon, Schrödinger operators in the twenty-first century, J. Math. Phys. **41**, 3523 (2000).

[51] B. Simon, Twelve tales in mathematical physics: An expanded Heinemann Prize lecture, arXiv:2011.12335.

[52] Y. Last,Exotic spectra: A review of Barry Simon's Spectral Theory and Mathematical Physics: A Festschrift in Honor of Barry Simon's 60th Birthday, Proceedings of Symposia in Pure Mathematics [Am. Math. Soc. **76**, 697 (2007)].

[53] E. I. Dinaburg and Y. G. Sinai, The one-dimensional Schrödinger equation with a quasiperiodic potential, Functional Anal. Appl. **9**, 279 (1976).

[54] S. Y. Jitomirskaya and Y. Last, Anderson localization for the almost Mathieu equation, III. Semi-uniform localization, continuity of gaps, and measure of the spectrum, Commun. Math. Phys. **195**, 1 (1998).

[55] A. Avila and S. Jitomirskaya, Hölder continuity of absolutely continuous spectral measures for one-frequency Schrödinger operators, Commun. Math. Phys. **301**, 563 (2011).

[56] X. Zhao, Hölder continuity of absolutely continuous spectral measure for multi-frequency Schrödinger operators, J. Funct. Anal. **278**, 108508 (2020).

[57] S. H. Amor, Holder continuity of the rotation number for quasi-periodic co-cycles in $(\mathrm{SL}(2,\mathbb{R}))$, Commun. Math. Phys. **287**, 565 (2009).

[58] F. Liu, S. Ghosh, and Y. D. Chong, Localization and adiabatic pumping in a generalized Aubry-André-Harper model, Phys. Rev. B **91**, 014108 (2015).